13èmes Journées de l'Hydrodynamique
21 - 23 novembre 2012
Laboratoire d'Hydraulique Saint-Venant
Ile des Impressionnistes,
Chatou (78), France

SIMULATION NUMERIQUE DU TSUNAMI GENERE PAR UN EBOULEMENT DU FLANC DU VOLCAN CUMBRE VIEJA (LA PALMA, CANARIES), PAR UNE APPROCHE COUPLEE NAVIER-STOKES / BOUSSINESQ

NUMERICAL SIMULATION OF THE TSUNAMI GENERATED BY THE CUMBRE VIEJA FLANK COLLAPSE (LA PALMA, CANARY) BY A COUPLED NAVIER-STOKES / BOUSSINESQ APPROACH

J.C. HARRIS*,, S.T. GRILLI**, S. ABADIE*****

* Now at Laboratoire Saint-Venant, Ecole des Ponts, 78401 CHATOU, *jcharris@oce.uri.edu*
** Department of Ocean Engineering, Univ. of Rhode Island, Narragansett, RI 02882, USA
*** SAIME EA 4581, Université de Pau et des Pats de l'Adour, 64600 ANGLET

Résumé

Plusieures études antérieures indiquent que l'éboulement à grande échelle du flanc du volcan Cumbre Vieja (CVV) sur l'île de La Palma (Iles Canaries) générerait un méga-tsunami qui pourrait potentiellement dévaster de nombreuses zones côtières de l'Atlantique nord. Dans ce travail, on présente une série de scénarios de tsunamis potentiels, sur la base d'études préalables de la stabilité des pentes du volcan, du mouvement de l'éboulement généré, et des vagues produites dans le champ proche [4]. Lors des simulations numériques, le modèle Navier-Stokes THETIS est utilisé pour la modélisation de l'éboulement et des vagues qu'il génère et le modèle Boussinesq FUNWAVE-TVD pour la modélisation de la propagation du tsunami, sous la forme d'un train d'ondes dispersives, dans une série de maillages emboités de résolution adéquate, pour le champ proche, la propagation dans l'océan Atlantique et le champ lointain. Dans ce travail, on présente de nouveaux résultats à haute résolution (1 min. d'arc) pour la propagation transocéanique, de même que le couplage unidirectionnel vers des maillages côtiers plus fins, pour la prévision de l'inondation et du runup dans les zones vulnérables. Les résultats sur des maillages de 4 sec. d'arc en zones côtières confirment la précision du schéma de couplage qui a été implémenté dans FUNWAVE-TVD.

Summary

Several earlier studies indicate that the large scale flank collapse of the Cumbre Vieja Volcano (CVV) on La Palma (Canary Islands) could generate a mega-tsunami, potentially devastating for many of the coastal areas of the North Atlantic Ocean. A detailed study of potential tsunami scenarios is presented herein, based on earlier studies of the volcanic

slope stability, generated landslide motion, and near-field wave motion [4]. In numerical simulations the Navier-Stokes model THETIS is used to model the landslide motion and resulting wave generation, and the Boussinesq model FUNWAVE-TVD to model the dispersive tsunami wave propagation in a variety of nested grids of adequate resolution, in the near-field, across the Atlantic Ocean, and in the far-field. In this paper, we present new results of transoceanic propagation at high resolution (1 arc-minute) as well as one-way coupling to finer coastal grids, for the prediction of inundation and runup in vulnerable areas. Coastal results in 4 arc-second resolution grids demonstrate the accuracy of the one-way coupling scheme that has been implemented in FUNWAVE-TVD.

I – Introduction

Recent catastrophic events (e.g., 2004 Indian Ocean, 2011 Tohoku) have dramatically demonstrated the risk faced by coastal communities due to tsunamis. While not as tsunami prone as other oceanic basins, one potential source of a major tsunami in the Atlantic Ocean is an extreme collapse of the western flank of the Cumbre Vieja Volcano (CVV ; if destabilized, e.g., due to a local earthquake/volcanic eruption), as suggested by Ward and Day [41] in their pioneering work. They considered a large 500 km^3 slide and, using simple models, predicted the generation of waves as large as 10-20 m off of the US east coast. Both the landslide parameters and model, and wave modeling, have since then been criticized and revisited by a number of authors [31, 34], but while more advanced models of the landslide generation [3] show smaller waves forming than originally suggested, these are still extremely large and hence the potential for a far-field coastal hazard could still exist and ought to be assessed.

Large landslides are in fact inherent to the volcanic building process, as material continuously accumulates until the point of slope failure [20]. Even small debris flows like the 0.5 km^3 Shimabara flank collapse in 1792 killed at least 4,000 people [21], and two consecutive landslides of O(1 km^3) (first underwater and second subaerial) during the Stomboli eruption of 2002 produced local runup of 10 m [40]. There is also clear geological evidence of past large paleo-submarine landslides of O(100 km^3) volume around the Canary Islands (Spain). Masson et al. [32] identified at least 14 large landslides, with the youngest one, at El Hierro, being only 15,000 years old. Such potentially catastrophic events may occur in average every 100,000 years in the Canary Archipelago. However, low probability does not necessarily mean low risk ; so for proper tsunami hazard assessment, the consequences associated with such catastrophic events must be carefully estimated and modeled.

The results below build upon our earlier results [3, 4, 18], which considered the landslide generation, near-field impact, and the amplitude of the waves within the Atlantic Ocean at a medium grid resolution. To pursue such simulations, we must make use of several different models and grids (Fig. 1). Here, we first perform higher resolution modeling of the propagation phase in the Atlantic (i.e., 1 arc-minute resolution instead of 2 arc-minute resolution of [18]), and also present some preliminary high-resolution (4 arc-second) results for a small coastal region of a distant coast (Myrtle Beach, USA), obtained by way of a new one-way coupling procedure.

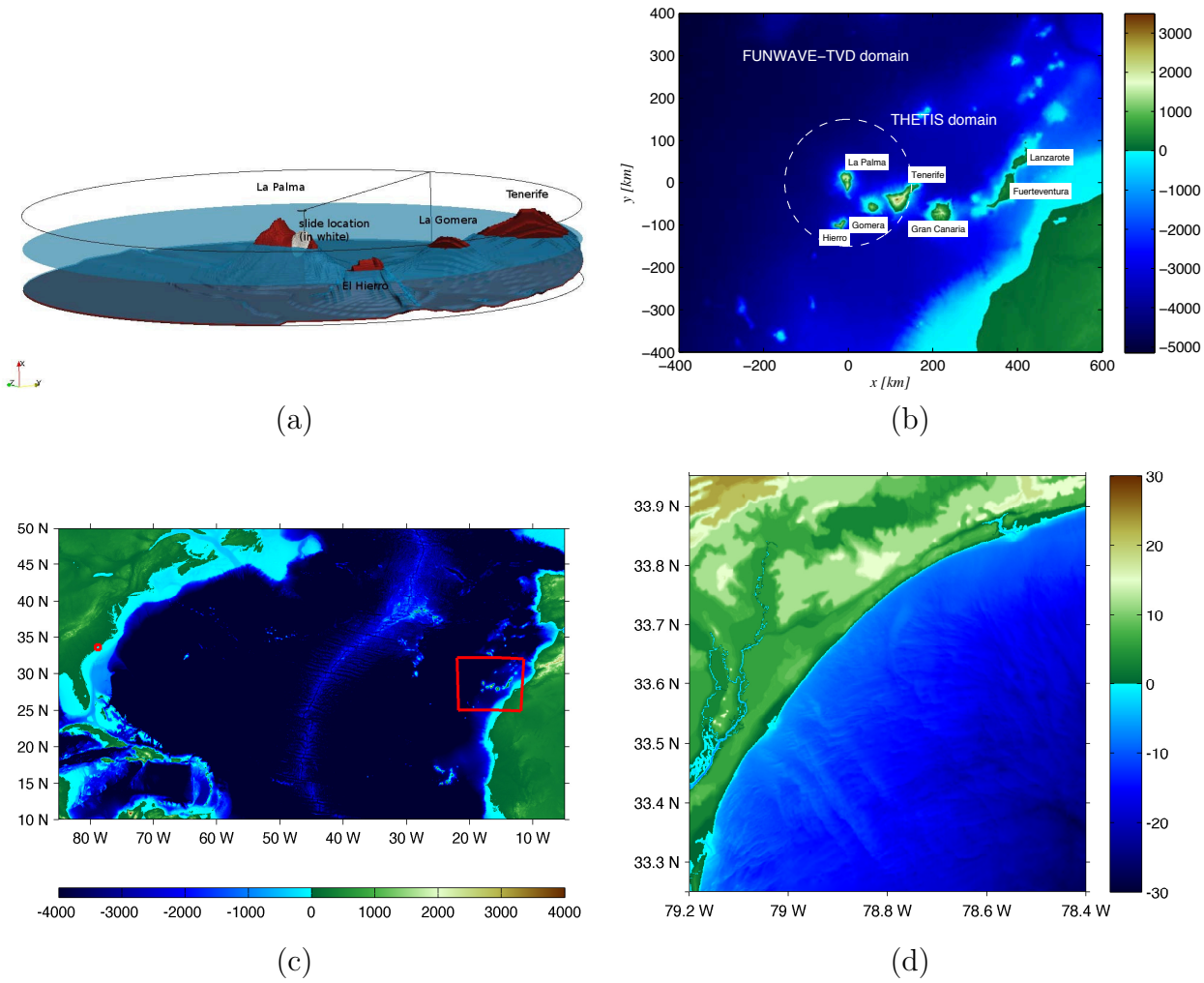

Figure 1 – Computational domains used for modeling the potential CVV events, including : (a) the higher resolution 3D THETIS domain surronding La Palma ; (b) the 500 m resolution FUNWAVE-TVD near-field domain ; (c) the 1 arc-minute resolution FUNWAVE-TVD Atlantic basin domain ; and (d) the 4 arc-second resolution FUNWAVE-TVD fine resolution coastal domain, to demonstrate coastal impact in the US (Myrtle Beach, SC). Red boxes in grid (c) indicate the boundary of grids (b) and (d).

II – Models

II – 1 THETIS

THETIS is a three-dimensional general purpose multi-fluid NS solver, developed over the past 15 years by the TREFLE CNRS laboratory at the University of Bordeaux, France. THETIS has been used to model wave generation from rigid or deforming slides [33, 5], but also is accurate to simulate plunging breaking waves [1, 30], which is important for accurately simulating initial waves due to violent subaerial slides. In THETIS, the air-water-slide domain is modeled as a single fluid, but one whose density and viscosity vary with space (using a penalty method). For this case, the incompressible NS equations are solved using a large-eddy simulation, where the water, air, and slide are represented as a single Newtonian fluid (though the model could easily use non-Newtonian laws to simulate the slide, such as the Herschel-Bulkley generalized model). In the present application,

turbulent dissipation is modeled using a mixed scale subgrid model [30]. The governing equations are discretized using the finite volume method on a fixed staggered grid. All fluid-fluid interfaces are tracked using the VOF method [19]. Details of the model, including validation for slide generated waves, are given by Abadie et al. [5].

A cylindrical mesh surrounding La Palma (Fig. 1) was used for these simulations, where the grid size grows with distance from the domain center, and the islands of El Hierro, La Gomera, and Tenerife have been included in the domain. The domain extends 8 km from top to bottom, and has a 150 km radius, with 80 grid cells vertically (stretched ; minimum spacing 10 m), 300 cells radially, and 140 cells in the tangential direction (stretched ; minimum spacing 1.4^o).

Based on earlier slope stability analyses [2, 10], four scenarios were considered : 40 and 80 km^3 slide volume scenarios considered consistent with the stability analysis, and two extreme cases, with 20 and 450 km^3, the latter being similar to that used by many authors when accounting for the more accurate geometry of the volcano represented here [41, 35, 12, 11, 29]. In this paper, we will consider the two largest slide volumes (i.e., a most-likely and a worst-case scenarios). For these cases, the debris flow is modeled as a constant 2,500 kg/m^3 density (corresponding to basalt). Basal friction is not specified, nor resistance to internal deformation, both of which would likely reduce the magnitude of the resulting tsunami. Results suggest that these factors are small in large rock slides, however [28].

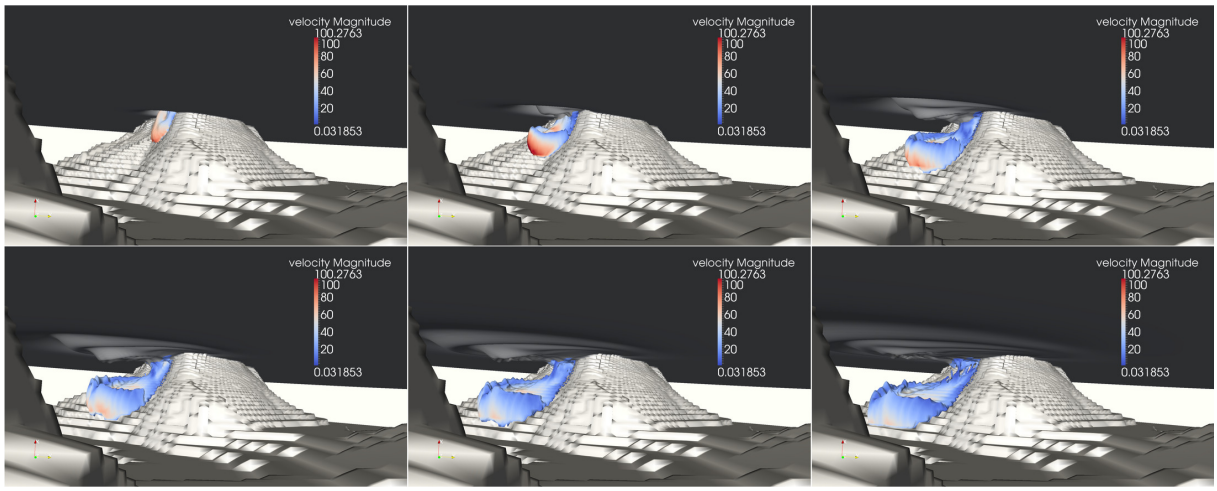

Figure 2 – Simulations of landslide tsunami generation with THETIS, for an initial slide volume of 80 km^3. Underwater views of water and slide interfaces (volume fractions respectively equal to 0.5 and 0.1) at t = a) 50 s, b) 100 s, c) 150 s, d) 200 s, e) 250 s, and f) 300 s.

Figure 2 shows results of THETIS simulations for the 80 km^3 CVV flank collapse scenario, consisting in six underwater snapshots for increasing time, displaying the air/water and water/slide interfaces. The 0.5 water volume fraction defines the air-water interface, while the 0.1 slide volume fraction defines the water/slide interface. [Note, the latter value was selected rather than 0.5 because, due to the combined effects of mixing and shearing, a 50% slide volume rate no longer occurs beyond some stage of slide motion.] The coupling between slide motion and free surface wave generation is quite clear on the figure, with first the generation of a large depression wave associated with the strong initial slide downward velocity, characteristic of large subaerial slides, and then the propagation of a train of cylindrical waves radiating away from the slide. Simulations indicate that, for a

long time, the slide nearly travels at the speed of the leading generated surface wave, allowing for a large transfer of its energy to waves. Tsunami directivity is approximately 24^o from west. As shown in Abadie et al. [4], the resulting waves are of intermediate depth, so frequency dispersion is important. Thus, a dispersive model must be used to simulate the transoceanic propagation and simulate waves in the far-field, as opposed to the traditional nonlinear shallow water equations usually used for co-seismic tsunami modeling.

II – 2 FUNWAVE-TVD

As a Navier-Stokes model would be too computationally costly and dissipative to use for simulating distant wave propagation, beyond the region directly surrounding La Palma, a 2D Boussinesq model FUNWAVE-TVD is used, which is initialized with the 3D THETIS model results. FUNWAVE-TVD is a recent improvement of the FUNWAVE model [43, 24, 7, 8, 25], which was originally developed and used for simulating coastal and nearshore waves, but was later successfully applied to a variety of tsunami case studies, both landslide and co-seismic [42, 9, 17, 22, 38, 23, 13]. FUNWAVE-TVD was developed as a fully nonlinear and dispersive model, first in Cartesian coordinates [36], and later in spherical coordinates with Coriolis effects [26, 27] approximation ; although formulated for full nonlinearity as well, the latter model has only been implemented so far as a weakly nonlinear approximation. Hence, since initial waves generated by the CVV slide and modeled in THETIS are strongly nonlinear, the Cartesian fully nonlinear model is first used for the simulations in the near-field coastal grids. Then, the weakly nonlinear spherical model is used for simulating the transoceanic propagation in the Atlantic Ocean basin scale grid (Fig. 1). FInally, for the nearshore coastal grids, along the US east coast, as nonlinearity becomes significant in shoaling waves, the fully nonlinear Cartesian model should again be used. However, at present, to more easily demonstrate our one-way coupling scheme, the spherical version is also used in a far-field 4 arc-second coastal grid. In the future, however, the Cartesian version will be used instead. It should be noted, the same Boussinesq models were successfully used to predict both far-field propagation [14] and coastal impact [16] of the recent 2011 Tohoku earthquake (see Grilli et al.'s paper in these proceedings).

While co-seismic tsunami propagation has traditionally been done using the nonlinear shallow water equations, tsunamigenic landslides such as in the present case produce shorter, dispersive wave trains and hence require non-hydrostatic or Boussinesq-type models for their accurate modeling. FUNWAVE-TVD is based on the equations of [6] and [36], which use a combined finite-volume and finite-difference MUSCL-TVD scheme. As in FUNWAVE [43], improved linear dispersive properties are achieved, up to the deep water limit, by expressing the BM equations in terms of the horizontal velocity vector at 0.531 times the local depth. FUNWAVE-TVD's latest implementation is fully parallelized using MPI, for efficient use on distributed memory clusters. This model was fully validated using all of NOAA's National Tsunami Mitigation Program (NTHMP) mandatory benchmarks in both Cartesian [39] and spherical [37] coordinates.

III – Coupling

The modeling of wave propagation for such a large range of scales, from landslide generation, deep water oceanic propagation, to inundation on a distant coast, requires using model grids a various resolution and geometry and hence a coupling scheme to accurately pass simulation results in real time from one model grid to another was developed.

III – 1 THETIS to FUNWAVE-TVD

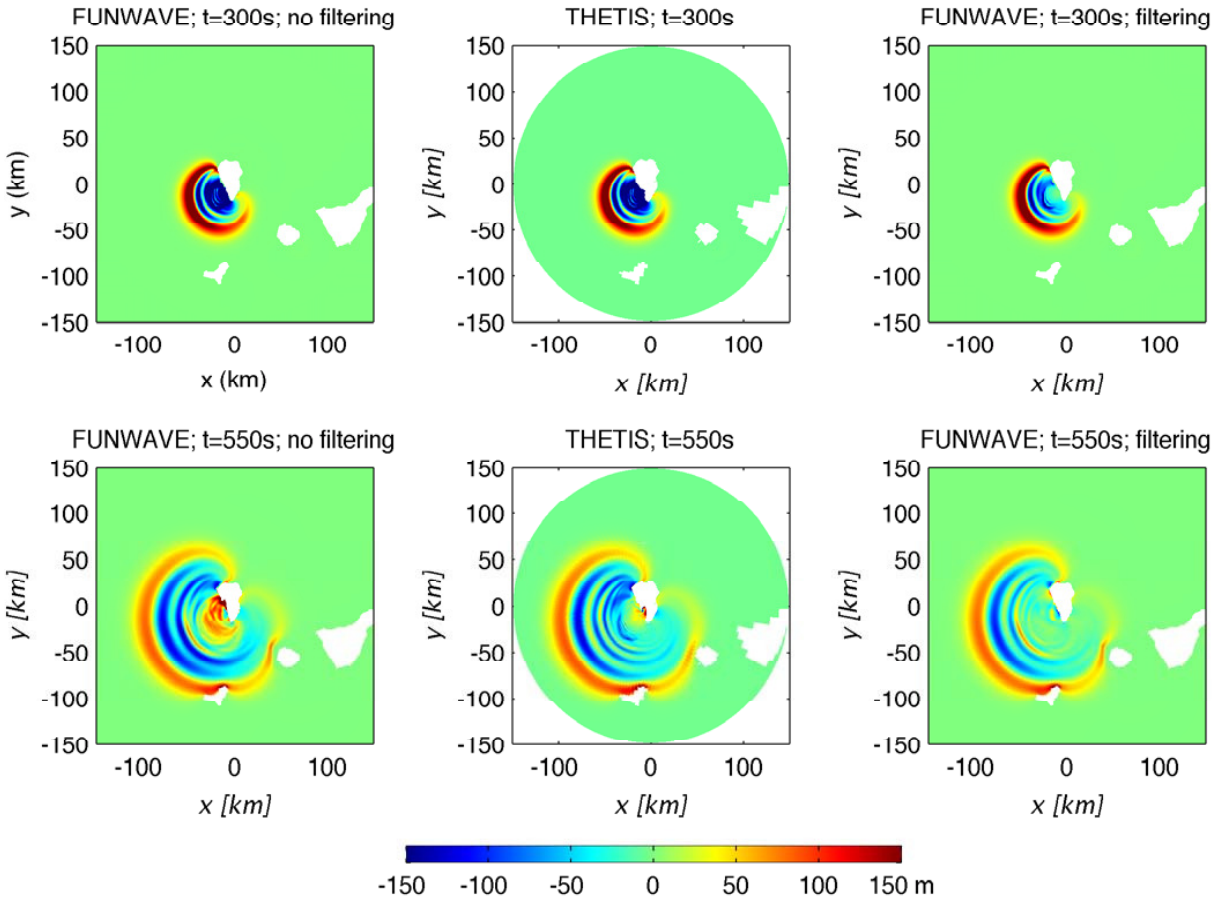

Figure 3 – Test of model coupling for the 80 km^3 case, when modeling wave propagation from $t = 300$ to 500 s, using : (i) FUNWAVE without filtering of the initial conditions ; (ii) THETIS ; and (iii) FUNWAVE with filtering of the initial conditions.

In order to transition from THETIS to FUNWAVE-TVD, the 3D-VOF-NS solution at $t = 300$ s is used as an initial condition for FUNWAVE. This time is selected as the leading edge of the tsunami has not yet reached the edge of the THETIS domain, and although there is still turbulent flow in the 3D domain, results show that all of the energy transfer from the slide to the tsunami waves has already occurred [3]. The NS velocity field is depth-averaged and the averaged horizontal velocity, together with the free surface elevation are interpolated onto the FUNWAVE mesh (which satisfies has conservation). This results in a slight error (2nd-order in kh), as the BM equations are framed in terms of a single horizontal velocity at a reference depth, but we verified this has little effect on the results and has the advantage of averaging out the turbulent flow in the vertical direction. In addition, the NS solution is further filtered near the slide motion prior to using it in FUNWAVE [3]. An ad hoc filtering method (Fig. 3) was determined through numerical experimentation, which consisted in multiplying the output of THETIS (i.e., free-surface elevation and each velocity component) by a spatially varying function, removing the interior flow while keeping a smooth initial condition for FUNWAVE. This function is Gaussian, with a standard deviation of 15 km and the origin located at coordinates (-10 km, -10 km).

Prior to performing longer-term propagation simulations in FUNWAVE, the authors verified that this coupling approach provided reasonable initial results, for at least the first few leading waves, since most of the near-field run-up and inundation will be caused by these waves, and, in the far-field, by waves originated from these waves through frequency dispersion. This was done by initializing FUNWAVE using THETIS results at $t = 300$ s and performing simulations with both models for an additional 250 s. To assess the effects of filtering THETIS results, FUNWAVE computations were performed using both unfiltered and filtered results. Free surface elevations computed in both models were then compared at $t = 550$ s. Fig. 3 shows results for the 80 km^3 case. Although FUNWAVE's unfiltered results appear reasonable as compared to THETIS', as expected, there is not enough near-shore dissipation of shorter waves, which stay in the back of the FUNWAVE train, but do not persist in THETIS results. Besides causing unrealistically large short waves to appear near La Palma, using unfiltered results also affects at least the 3rd leading wave in the tsunami train. This is greatly improved in FUNWAVE's filtered results, which compare well to THETIS' ; both the large short waves near La Palma dissipate and the 3rd leading wave now agrees well with THETIS results. Similar results are seen for the other slide volumes.

III – 2 FUNWAVE-TVD : fine grid to coarse grid

For moving from a small, fine grid (e.g., to model the source area) to a coarse grid (e.g., for transoceanic propagation), results are simply interpolated in space – i.e., at a set time, the results from the fine grid are interpolated to the larger grid, which includes the wave elevation and horizontal velocity in both the north/south and east/west directions, as a "hot-start" initial condition.

In order to prevent aliasing effects from changing resolution, the results on the finer grid are first filtered with a box filter with a filter width equal to that of the coarse grid.

III – 3 FUNWAVE-TVD : coarse grid to fine grid

For dynamically moving from a coarse grid to a finer grid, a one-way coupling scheme was developed. Boundary conditions are used in the form of time series computed in the coarse grid for a series of "numerical wave gages" corresponding to the cells of the outer boundary of the fine grid. We usually start simulating in the fine grid early enough in time, such that the domain is initially at rest (i.e., the incoming tsunami is barely reaching its outer boundary). Specifically, here, in the coarser 1' grid over the ocean basin (e.g., Fig. 1c), a series of numerical wave gauges are setup, where time series of water elevation and velocity are computed along the boundaries of the 4" fine grid off of Myrtle Beach. These results are linearly interpolated in space and time to provide the boundary values for the finer grid.

We can test that the results are accurate by comparing the results between the two grids for the same times (Fig. 4), when waves are still fairly offshore (and hence not too affected by the nearshore bathymetry) in this case at 9h20' after the CVV event. Following transoceanic propagation, the finer grid simulations were initiated at 8h20' after the start of the CVV event (hence one additional hour of propagation has already taken place in the fine grid). We see that the wave amplitude wavelength, direction, all are approximately the same in both coarse and fine grids, although there is already some wave steepening in the finer grid as a result of the more finely resolved bathymetry and grid. From this and similar comparisons, we see that this one-way coupling scheme provides the correct wave

information to the finer domain.

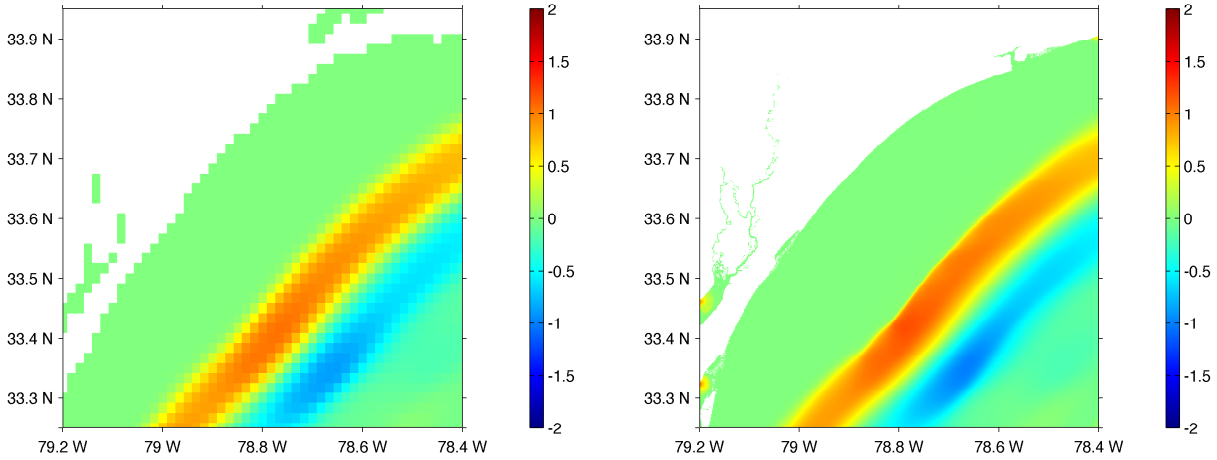

(a) (b)

Figure 4 – Comparison of wave elevation at 9h20' after the start of the CVV event (including 5' of THETIS and 15' of 500 m resolution FUNWAVE-TVD modeling) as predicted for the (a) coarse, 1 arc-minute resolution domain, and the (b) finer, 4 arc-second resolution domain.

IV – Distant effects

IV – 1 Transatlantic propagation

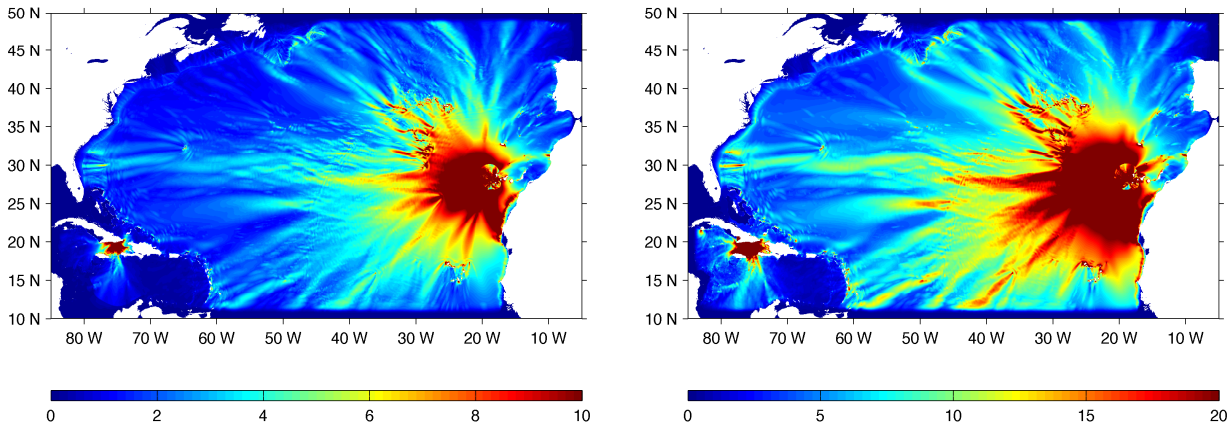

(a) (b)

Figure 5 – Maximum surface elevation in meters for the 1 arc-minute resolution Atlantic grid, for both the (a) 80 km^3 and (b) 450 km^3 CVV slide scenarios. [Note that the high elevations in the Caribbean are from non-physical numerical instabilities at the wetting-drying boundary due to low resolution.]

After modeling the initial slide in THETIS for 5 min., and on the regional (500 m) grid with FUNWAVE for an additional 15 min., the leading wave train is sufficiently long

to be accurately resolved on a coarser 1 arc-minute grid that covers the North Atlantic (Fig. 5), from 10^o to 50^o N, and from 85^o to 5^o W. The bathymetry for this domain is taken from ETOPO1. The simulation of the propagation with FUNWAVE shows that large waves, several meters high, would reach shorelines of the US, Europe and Africa (in the latter case, waves would be much larger owing to proximity). Figure 5 shows the maximum wave elevation in the Atlantic computed for both the 80 and 450 km^3 CVV slide scenarios. Clearly either tsunami would have damaging effects for large low-lying coastal areas and cities all along the Atlantic basin, including northwest Africa, western Europe, and eastern North America. [Note, the high waves seen in the Caribbean result from a numerical instability at the wetting-drying interface due to the low resolution, but does not affect the results elsewhere.]

IV – 2 Far-field coastal impact

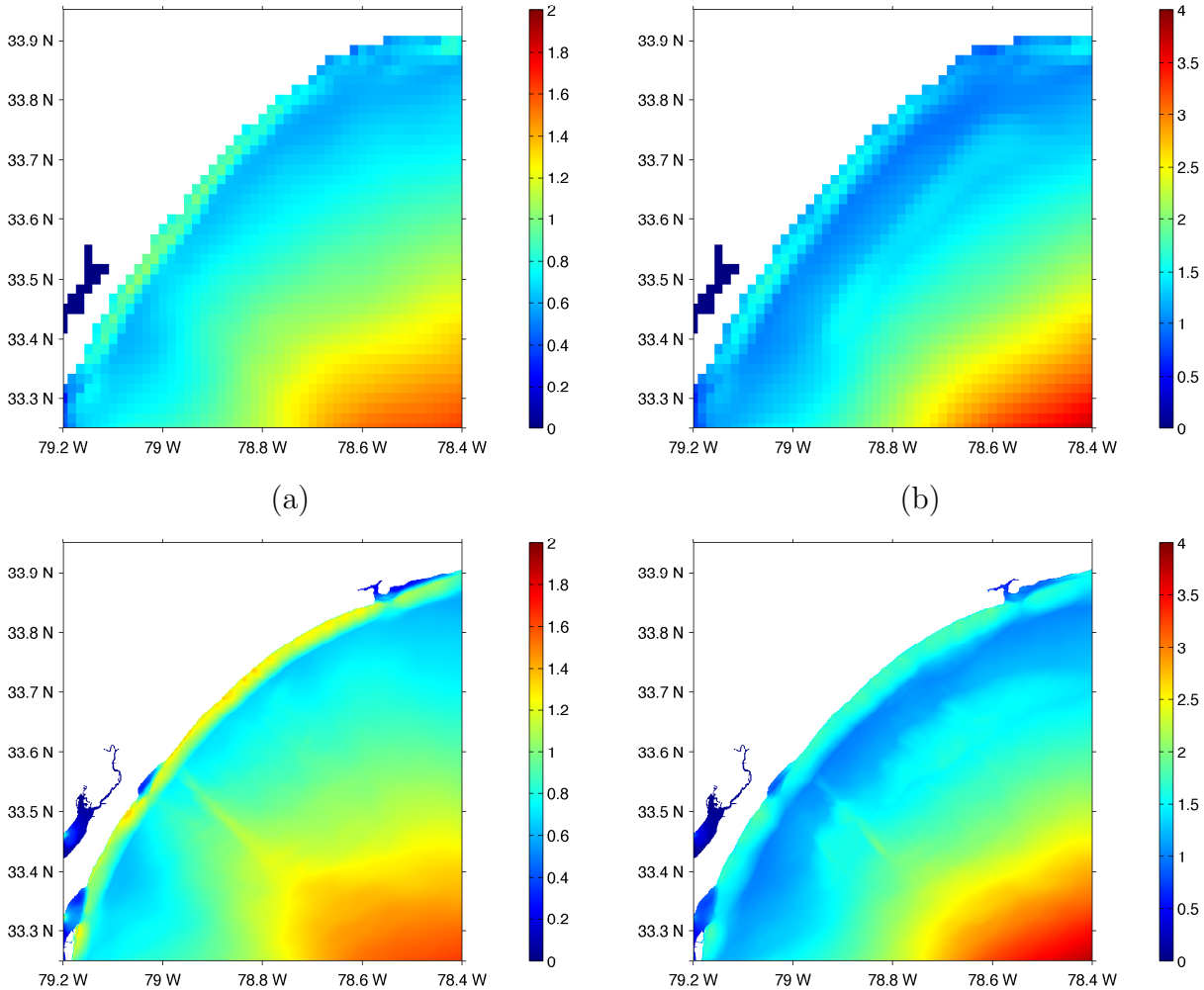

Figure 6 – Comparison of maximum surface elevation predicted at Myrtle Beach, SC, for the 80 and 450 km^3 CVV slide scenarios, on the 1' grid (a ; b), and on the 4" grid (c ; d).

Accurately predicting tsunami coastal impact is only possible with high-resolution modeling of the various nearshore wave transformations, breaking and dissipation that

take place. This would be computationally prohibitive while simultaneously modeling an ocean basin with a structured grid (i.e., same resolution everywhere). Instead, nested grids of decreasing resolution are used as detailed before. Unlike earlier work [18], here we make use of a recently developed one-way coupling scheme, through applying time-varying boundary conditions, as described above. Previous work simply used an initial condition, so the nearshore domains had to extend out far into the ocean to capture the leading tsunami waves of the tsunami arriving from the coarser grid in the simulation.

Here we consider a 4 arc-second grid from 33.25^o to 33.95^o N and from 79.2 to 78.4^o W, corresponding to the domain of the Myrtle Beach tsunami DEM (digital elevation model) to be used for predicting tsunami inundation in the region. The bathymetry used is from the 3 arc-second resolution NOAA Coastal Relief Model, though for future modeling higher-resolution data is available for the region. [Note, a rule of thumb of gradually reducing the grid mesh by a factor of 4 was developed in our earlier work, which we violate here, for the purpose of illustration, by nesting to a fine grid with a factor of 15 in mesh reduction.] Figure 6 shows a comparison of the 1 arc-minute and 4 arc-second results for the 80 and 450 km^3 CVV slide scenarios, demonstrating that the general pattern of results is similar for the two resolutions, but as could be expected the amplitude of the waves along the coastline is higher in the finer resolution grid results, a sign that the 1 arc-minute grid is too coarse to accurately capture the coastal bathymetry and wave processes.

Note that the wave elevation decreases as it approaches the shoreline, which is unusual. While along shallow continental shelves in other situations this anomalous dissipation could be due to the appearance of a breaking bore, where the simple breaking model of FUNWAVE-TVD may not provide accurate results [15], here there is no sign of such breaking. It could, however, be caused by the extremely large aspect ratio (1 :15) between grid spacing and water depth that is used in these simulations, causing unwanted numerical diffusion. More careful nesting of model grids will be used in future work, using in particular additional intermediate levels of grid nesting.

V – Conclusions

Two scenarios of the potential Cumbre Vieja Volcano (CVV) flank collapse were simulated, including the landslide tsunami generation, propagation, and far-field impact. THETIS, a multi-fluid Navier-Stokes 3D solver with VOF interface tracking, was first used to calculate the free surface and water velocity generated by the deforming slide motion resulting form the CVV flank collapse. Then, FUNWAVE-TVD, a Boussinesq wave model, was used in a series of nested grids to compute the oceanic propagation and far-field impact of the potential tsunami along the US East Coast. A new accurate one-way compiling scheme between model grids was developed and validated in the process.

This work extends our earlier work by considering higher resolution grids and more efficient one-way coupling of different model grids. It is part of current work being performed for the NOAA-NTHMP program, to develop tsunami inundation maps for the vulnerable areas of the US East coast, due to all the potential far-field and near-field tsunami sources.

Future model improvements will consider potential problems that arise from using different grid resolutions that may artificially affect the dissipation rate nearshore.

Références

[1] S. Abadie, J. P. Caltagirone, and P. Watremez. Splash-up generation in a plunging breaker. *Comptes Rendus de l'Academie des Sciences Series IIB*, 326 :553–559, 1998.

[2] S. Abadie, C. Gandon, S. Grilli, R. Fabre, J. Riss, E. Tric, D. Morichon, and S. Glockner. 3D numerical simulations of waves generated by subaerial mass failures. Applicaiton to La Palma case. In *Proceedings of the 31st International Coastal Engineering Conference*, 2008.

[3] S. Abadie, J. Harris, and S. Grilli. Numerical simulation of tsunami generation by the potential flank collapse of the Cumbre Vieja volcano. In *Proceedings of the 21st Offshore and Polar Engineering Conference*, 2011.

[4] S. Abadie, J. Harris, S. Grilli, and R. Fabre. Numerical modeling of tsunami waves generated by the flank collapse of the Cumbre Vieja Volcano (La Palma, Canary Islands) : tsunami source and near field effects. *Journal of Geophysical Research*, 117 :C05030, 2012.

[5] S. Abadie, D. Morichon, S. Grilli, and S. Glockner. Numerical simulation of waves generated by landslides using a multiple-fluid Navier-Stokes model. *Coastal Engineering*, 57 :779–794, 2010.

[6] Q. Chen. Fully nonlinear Boussinesq-type equations for waves and currents over porous beds. *Journal of Engineering Mechanics*, 132 :220–230, 2006.

[7] Q. Chen, J. T. Kirby, R. A. Dalrymple, A. B. Kennedy, and A. Chawla. Boussinesq modeling of wave transformation, breaking, and runup. II : 2-D. *Journal of Waterway, Port, Coastal, and Ocean Engineering*, 126 :48–56, 2000.

[8] Q. Chen, J. T. Kirby, R. A. Dalrymple, F. Shi, and E. B. Thornton. Boussinesq modeling of longshore currents. *Journal of Geophysical Research*, 108 :3362, 2003.

[9] S. J. Days, P. Watts, S. T. Grilli, and J. T. Kirby. Mechanical models of the 1975 Kalapana, Hawaii earthquake and tsunami. *Marine Geology*, 215 :59–92, 2005.

[10] R. Fabre, J. Riss, E. Tric, T. Lebourg, and S. Abadie. Potential collapse of the Cumbre Vieja volcanic edifice (La Palma Island, Spain) : numerical investigation of the failure model and potential volume. *Engineering Geology*, (submitted), 2011.

[11] G. Gisler, R. Weaver, and M. Gittings. SAGE calculations of the tsunami threat from La Palma. *Science of Tsunami Hazards*, 24 :288–301, 2006.

[12] S. T. Grilli, C. D. P. Baxter, S. Maretzki, Y. Perignon, and D. Gemme. Numerical simulation of tsunami hazard maps for the US East Coast. Report of Year 1 project. FMGlobal Project. Technical report, University of Rhode Island, 2006.

[13] S. T. Grilli, S. Dubosq, N. Pophet, Y. Perignon, J. T. Kirby, and F. Shi. Numerical simulation and first-order hazard analysis of large co-seismic tsunamis generated in the Puerto Rico thrench : near-field impact on the North shore of Puerto Rico and far-filed impact on the US East Coast. *Natural Hazards and Earth System Sciences*, 10 :2109–2125, 2010.

[14] S. T. Grilli, J. C. Harris, T. T. Bakhsh, T. L. Masterlark, C. Kyriakopolos, J. T. Kirby, and F. Shi. Numerical simulation of the 2011 Tohoku tsunami based on a new transient FEM co-seismic source : comparison to far- and near-field observations. *Pure and Applied Geophysics*, (published online) :27 pp., 2012.

[15] S. T. Grilli, J. C. Harris, F. Shi, J. T. Kirby, T. S. T. Bakhsh, E. Estibals, and B. Tehranirad. Numerical modeling of coastal tsunami dissipation and impact. In *Proceedings of the 33rd International Coastal Engineering Conference*, 2012.

[16] S. T. Grilli, J. C. Harris, D. Tappin, T. L. Masterlark, J. T. Kirby, F. Shi, and G. Ma. A multi-source origin for the Tohoku-oki 2011 tsunami earthquake and seabed failure. *Nature Communications*, (submitted), 2012.

[17] S. T. Grilli, M. Ioualalen, J. Asavanant, F. Shi, J. Kirby, and P. Watts. Source constraints and model simulation of the December 26, 2004 Indian Ocean tsunami. *Journal of Waterway, Port, Coastal, and Ocean Engineering*, 33 :414–428, 2007.

[18] J. C. Harris, S. T. grilli, S. Abadie, and T. T. Bakhsh. Near- and far-field tsunami hazard from the potential flank collapse of the Cumbre Vieja Volcano. In *Proceedings of the 22nd Offshore and Polar Engineering Conference*, 2012.

[19] C. W. Hirt and B. D. Nichols. Volume of fluid (VOF) method for the dynamics of free boundaries. *Journal of Computational Physics*, 39 :201–225, 1981.

[20] R. T. Holcomb and R. C. Searle. Large landslides from oceanic volcanoes. *Marine Geotechnology*, 10 :19–32, 1991.

[21] K. Inoue. Shimabara-Shigatusaku Earthquake and topographic changes by Shimabara Catastrophe in 1792. *Geographical Reports of Tokyo Metropolitan University*, 35 :59–69, 2000.

[22] M. Ioualalen, J. Asavanant, N. Kaewbanjak, S. T. Grilli, J. T. Kirby, and P. Watts. Modeling the 26th December 2004 Indian Ocean tsunami : Case study of impact in Thailand. *Journal of Geophysical Research*, 112 :C07024, 2007.

[23] J. M. Karlsson, A. Skelton, M. Sanden, M. Ioualalen, N. Kaewbanjak, N. Pophet, J. Asavanant, and A. von Matern. Reconstructions of the coastal impact of the 2004 Indian Ocean tsunami in the Khao Lak area, Thailand. *Journal of Geophysical Research*, 114 :C10023, 2009.

[24] A. B. Kennedy, Q. Chen, J. T. Kirby, and R. A. Dalrymple. Boussinesq modeling of wave transformation, breaking, and runup. I : 1D. *Journal of Waterway, Port, Coastal, and Ocean Engineering*, 126 :39–47, 2000.

[25] J. T. Kirby. *Advances in Coastal Modeling*, chapter Boussinesq models and applications to nearshore wave propagation, surf zone processes and wave-induced currents, pages 1–41. Elsevier, 2003.

[26] J. T. Kirby, N. Pophet, F. Shi, and S. T. Grilli. Basin scale tsunami propagation modeling using Boussinesq models : Parallel implementation in spherical coordinates. In *Proceedings of the WCCE-ECCE-TCCE Joint Conference on Earthquake and Tsunami*, volume paper 100, page (published on CD), 2009.

[27] J. T. Kirby, F. Shi, J. C. Harris, and S. T. Grilli. Sensitivity analysis of trans-oceanic tsunami propagation to dispersive and Coriolis effects. *Ocean Modelling*, (accepted) :42 pp., 2012.

[28] F. Legros. The mobility of long-runout landslides. *Engineering Geology*, 63 :301–331, 2002.

[29] F. Løvholt, G. Pedersen, and G. Gisler. Oceanic propagation of a potential tsunami from the La Palma Island. *Journal of Geophysical Research*, 113 :C09026, 2008.

[30] P. Lubin, S. Vincent, S. Abadie, and J. P. Caltagirone. Three-dimensional large eddy simulation of air entrainment under plunging breaking waves. *Coastal Engineering*, 53 :631–655, 2006.

[31] C. L. Mader. Modeling the La Palma landslide tsunami. *Science of Tsunami Hazards*, 19 :150–170, 2001.

[32] D. Masson, A. Watts, M. Gee, R. Urgeles, N. Mitchell, T. L. Bas, and M. Canals. Slope failures on the flanks of the western Canary Islands. *Earth-Science Reviews*, 57 :1–35, 2002.

[33] D. Morichon and S. Abadie. Vague générée par un glissement de terrain, influence de la forme initiale et de la loi de déformabilité du glissement. *La Houille Blanche*, 1 :111–117, 2010.

[34] G. Pararas-Carayannis. Evaluation of the threat of mega tsunamis generation from postulated massive slope failures of island strato-volcanoes on La Palma, Canary Islands, and on the island of Hawaii. *Science of Tsunami Hazards*, 20 :251, 2002.

[35] Y. Pérignon. Tsunami hazard modeling. Master's thesis, University of Rhode Island and Ecole Centrale de Nantes, 2006.

[36] F. Shi, J. T. Kirby, J. C. Harris, J. D. Geiman, and S. T. Grilli. A high-order adaptive time-stepping TVD solver for Boussinesq modeling of breaking waves and coastal inundation. *Ocean Modelling*, 43-44 :36–51, 2012.

[37] F. Shi, J. T. Kirby, and B. Tehranirad. Tsunami benchmark results for spherical coordinate version of FUNWAVE-TVD (Version 1.1). Technical report, No. CACR-12-02, Center for Applied Coastal Research, University of Delaware, 2012.

[38] D. R. Tappin, P. Watts, and S. T. Grilli. The Papua New Guinea tsunami of 1998 : anatomy of a catastrophic event. *Natural Hazards and Earth System Sciences*, 8 :243–266, 2008.

[39] B. Tehranirad, F. Shi, J. T. Kirby, J. C. Harris, and S. T. Grilli. Tsunami benchmark results for fully nonlinear Boussinesq wave model FUNWAVE-TVD, Version 1.0. Technical report, No. CACR-11-02, Center for Applied Coastal Research, University of Delaware, 2011.

[40] S. Tinti, A. Manucci, G. Pagnoni, A. Armigliato, and F. Zaniboni. The 30th December 2002 landslide-induced tsunami in Stromboli : sequence of the events reconstructed from eyewitness accounts. *Natural Hazards and Earth System Sciences*, 5 :763–775, 2005.

[41] S. N. Ward and S. Day. Cumbre Vieja Volcano – potential collapse at La Palma, Canary Islands. *Geophysical Research Letters*, 28 :397–400, 2001.

[42] P. Watts, S. T. Grilli, J. T. Kirby, G. J. Fryer, and D. R. Tappin. Landslide tsunami case studies using a Boussinesq model and a fully nonlinear tsunami generation model. *Natural Hazards and Earth System Sciences*, 3 :391–402, 2003.

[43] G. Wei, J. T. Kirby, S. T. Grilli, and R. Subramanya. A fully nonlinear Boussinesq model for free surface waves. Part I : Highly nonlinear unsteady waves. *Journal of Fluid Mechanics*, 294 :71–92, 1995.